cmgh
CELLULAR AND MOLECULAR GASTROENTEROLOGY AND HEPATOLOGY

ORIGINAL RESEARCH

BET Inhibition Rescues Acinar-Ductal-Metaplasia and Ciliogenesis and Ameliorates Chronic Pancreatitis-Driven Changes in Mice with Loss of the Polarity Protein Par3

Mario A. Shields,[1,2] Anastasia E. Metropulos,[1,3] Christina Spaulding,[1,3] Khulood A. Alzahrani,[1] Tomonori Hirose,[4,5] Shigeo Ohno,[4] Thao N. D. Pham,[1,2] and Hidayatullah G. Munshi[1,2,3]

[1]Department of Medicine, Feinberg School of Medicine, Northwestern University, Chicago, Illinois; [2]The Robert H. Lurie Comprehensive Cancer Center, Chicago, Illinois; [3]Jesse Brown VA Medical Center, Chicago, Illinois; [4]Department of Molecular Biology, Yokohama City University School of Medicine, Yokohama, Japan; and [5]Department of Cell Biology, Cancer Institute, Japanese Foundation for Cancer Research, Tokyo, Japan

SUMMARY

This study increases the understanding of the role of the polarity protein Par3 in restraining chronic pancreatitis-driven phenotypic changes. It also identifies BET inhibitors to attenuate pancreas injury and facilitate tissue regeneration in the context of Par3 loss.

BACKGROUND & AIMS: The apical-basal polarity of pancreatic acinar cells is essential for maintaining tissue architecture. However, the mechanisms by which polarity proteins regulate acinar pancreas injury and regeneration are poorly understood.

METHODS: Cerulein-induced pancreatitis was induced in mice with conditional deletion of the polarity protein Par3 in the pancreas. The impact of Par3 loss on pancreas injury and regeneration was assessed by histologic analyses and transcriptional profiling by RNA sequencing. Mice were pretreated with the bromodomain and extraterminal domain (BET) inhibitor JQ1 before cotreatment with cerulein to determine the effect of BET inhibition on pancreas injury and regeneration.

RESULTS: Initially, we show that Par3 is increased in acinar-ductal metaplasia (ADM) lesions present in human and mouse chronic pancreatitis specimens. Although Par3 loss disrupts tight junctions, Par3 is dispensable for pancreatogenesis. However, with aging, Par3 loss results in low-grade inflammation, acinar degeneration, and pancreatic lipomatosis. Par3 loss exacerbates acute pancreatitis-induced injury and chronic pancreatitis-induced acinar cell loss, promotes pancreatic lipomatosis, and prevents regeneration. Par3 loss also results in suppression of chronic pancreatitis-induced ADM and primary ciliogenesis. Notably, targeting BET proteins attenuates chronic pancreatitis-induced loss of primary cilia and promotes ADM in mice lacking pancreatic Par3. Targeting BET proteins also attenuates cerulein-induced acinar cell loss and enhances recovery of acinar cell mass and body weight of mice lacking pancreatic Par3.

CONCLUSIONS: Combined, this study demonstrates how Par3 restrains chronic pancreatitis-induced changes in the pancreas and identifies a potential role for BET inhibitors to attenuate pancreas injury and facilitate regeneration. *(Cell Mol Gastroenterol Hepatol 2024;18:101389; https://doi.org/10.1016/j.jcmgh.2024.101389)*

Keywords: Par3; Inflammation; ADM; Primary Cilia; BET Inhibitors.

Animal studies have shown that the exocrine pancreas possesses an intrinsic capacity for regeneration.[1,2] Induction of chronic pancreatitis results in acinar cells losing their differentiation and acquiring a duct-like state in a process called acinar-to-ductal metaplasia (ADM).[1–5] ADM protects against tissue damage and facilitates acinar pancreas regeneration after the resolution of the inflammatory stimulus.[1–5] Epigenetic programs regulate ADM, resulting in silencing of markers of acinar cell identity and activation of drivers of acinar cell dedifferentiation.[3,4] Epigenetic factors can impact the ADM program and modulate acinar injury and/or regeneration.[6,7] For example, a member of the bromodomain and extraterminal domain (BET) family of proteins, which are "readers" of histone acetylation marks,[8,9] regulates ADM and pancreas regeneration following induction of chronic pancreatitis.[6]

ADM is also associated with changes in cell polarity,[3,4,10] which plays a critical role in establishing cellular architecture and function.[11,12] Proper maintenance of cell polarity is necessary for tissue integrity because cell polarity prevents damage and preserves tissue homeostasis.[13–15] Concomitantly, reorganization of cell polarity during ADM promotes primary ciliogenesis, which is critical for coordinating developmental signaling processes important for regeneration.[16–18] Importantly, loss of pancreatic primary cilia results in pancreatitis and fatty changes.[19,20]

Several polarity programs control epithelial polarization and morphogenesis.[11,12] For example, the Par3 complex

Abbreviations used in this paper: **ADM, acinar-ductal-metaplasia; Arl13b, ADP ribosylation factor like GTPase 13B; BET, bromodomain and extraterminal domain; CK19, cytokeratin 19; Par3, partitioning defective protein-3.**

Most current article

2352-345X
https://doi.org/10.1016/j.jcmgh.2024.101389

(comprising partitioning-defective [Par]3, the atypical protein kinase C, and Par6) plays an essential role in controlling the apical domain identity.[13–15] Accordingly, loss of Par3 in the skin reduces self-renewal, increases differentiation, and causes premature skin aging.[21] Despite the importance of Par3 in skin homeostasis,[21,22] the role of Par3 in acinar pancreas has not been studied previously.

In this report, we evaluate the role of Par3 in acinar pancreas injury and homeostasis. Although Par3 loss in the mouse pancreas disrupts tight junctions, Par3 is dispensable for pancreatogenesis. However, with aging, Par3 loss results in low-grade inflammation, acinar degeneration, and pancreatic lipomatosis. Although Par3 loss exacerbates cerulein-induced acute and chronic pancreatitis, Par3 loss results in extensive acinar cell degeneration, pronounced pancreatic lipomatosis, and failure to regenerate with induction of chronic pancreatitis. We also show that Par3 loss restricts chronic pancreatitis-induced ADM and primary ciliogenesis. Significantly, the BET inhibitor JQ1 enhances primary ciliogenesis and ADM and limits chronic pancreatitis-induced acinar loss and facilitates acinar cell regeneration in mice with Par3 loss. Combined, this study demonstrates how Par3 restrains pancreatitis-induced changes in the pancreas and identifies a potential role for BET inhibitors to attenuate pancreas injury and facilitate pancreas tissue regeneration.

Results

Increased Par3 Expression in Human and Mouse Chronic Pancreatitis Specimens

Although there are changes in the apical-basal cell polarity during ADM,[3,4,10] the role of polarity proteins in the acinar pancreas homeostasis is yet to be fully understood. Here, we evaluate the role of the polarity protein Par3 in acinar pancreas homeostasis. Initially, we evaluated the expression of Par3 in chronic pancreatitis specimens using a previously validated Par3 antibody and human tissue microarray slides containing human pancreatitis sections. Compared with the mild and acute pancreatitis specimens, we found increased expression of Par3 in the chronic pancreatitis specimens (Figure 1*A*). Furthermore, we found increased expression of Par3 in ADM lesions present in the human chronic pancreatitis specimens compared with the surrounding pancreas (Figure 1*B*).

We also assessed Par3 expression in mouse pancreatitis specimens. Mice were treated with 8 hourly injections of cerulein to induce acute pancreatitis or twice daily for 5 days to induce chronic pancreatitis. Although induction of acute pancreatitis did not increase Par3 expression (Figure 1*C*), we found increased expression of Par3 in the chronic pancreatitis specimens compared with the surrounding pancreas (Figure 1*D*). When we costained the chronic pancreatitis specimens for amylase, cytokeratin 19 (CK19), and Par3, we show increased Par3 expression in the ADM lesions present in the mouse chronic pancreatitis specimens compared with the surrounding pancreas (Figure 1*E*).

Mice with Pancreatic Par3 Loss Exhibit Low-Grade Inflammation and Acinar Cell Loss with Aging

To evaluate the role of Par3 in vivo, we crossed Par3fl/+ mice with Pdx1-Cre mice to generate Pdx1-Cre x Par3fl/+ (CPar3fl/+) mice, which were then further crossed to obtain Pdx1-Cre x Par3fl/fl (CPar3fl/fl) mice (Figure 2*A*). There was a decreased pancreatic expression of Par3 and the tight junction protein Zo-1 in the CPar3fl/fl mice (Figure 2*B*). However, Par3 loss did not affect overall expression of the adherens junction protein E-cadherin in the CPar3fl/fl mice (Figure 2*B*). At 3 and 6 months of age, although there was minimal to no difference in the body weights between the CPar3+/+ mice and the CPar3fl/fl mice, the CPar3fl/fl mice exhibited reduced pancreas weights (Figure 2*C*). In addition, although there was not a gross difference in the acinar architecture, ductal structures, or pancreatic islets between the CPar3fl/fl and the CPar3+/+ mice at 3 months of age, there was evidence for loss of acinar cell mass in the CPar3fl/fl at 6 months of age (Figure 2*D*). Moreover, at 12 months of age, more than 50% (5/9; $P = .09$, Fisher exact test) of the CPar3fl/fl mice exhibited loss of acinar cells and increase in fat accumulation in the pancreatic parenchyma (pancreatic lipomatosis; Figure 2*E*). When we evaluated for inflammation, there was an increased presence of macrophages (F4/80) in the CPar3fl/fl mice at 3 and 6 months of age (Figure 2*F*).

Pancreatic Par3 Loss Results in Exacerbation of Cerulein-Induced Acute Pancreatitis

Given the presence of low-grade pancreatic inflammation in the CPar3fl/fl mice with aging, we evaluated the effects of Par3 loss on acinar cell injury with acute pancreatitis in 2- to 3-month-old mice (Figure 3*A*). Hematoxylin and eosin staining of the pancreas showed Par3 loss exacerbated cerulein-induced acute pancreatitis, as demonstrated by increased vacuolization, interlobular edema, and a more pronounced disruption of the acinar pancreas (Figure 3*A*). We also examined the effects of Par3 loss on cerulein-induced inflammation by staining for macrophages (F4/80) and neutrophils (Ly-6B.2, clone 7/4) in the Day 1 samples. Although we saw minimal numbers of neutrophils in the pancreas of both CPar3fl/fl mice and CPar3+/+ mice, we found there were more macrophages in the pancreas of CPar3fl/fl mice than that in the pancreas of CPar3+/+ mice (Figure 3*B*). In the Day 1 samples, the pancreas of CPar3fl/fl mice had significantly increased acinar cell proliferation and a significant but minimal increase in apoptosis (Figure 3*C*). These results indicate that although Par3 loss results in increased inflammation and damage, there is also increased acinar proliferation in the pancreas with Par3 loss, enabling regeneration of the acinar pancreas. However, there was also evidence for pancreatic lipomatosis in CPar3fl/fl mice following recovery from acute pancreatitis (Figure 3*D*), suggesting that the pancreas of CPar3fl/fl mice does not fully regenerate.

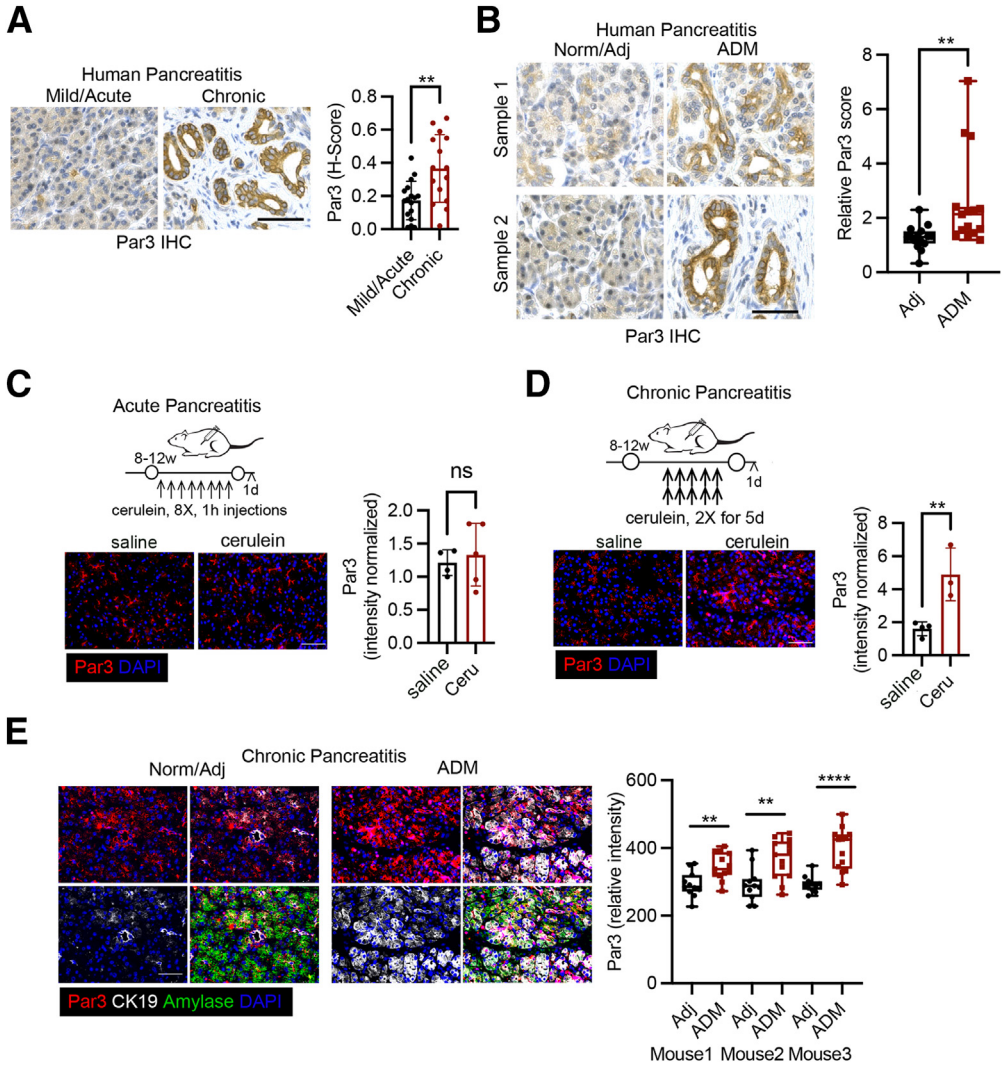

Figure 1. Increased Par3 expression in human and mouse chronic pancreatitis specimens. (*A*) Human pancreatitis tissue array was stained for Par3 by immunohistochemistry. Par3 expression in the mild/acute pancreatitis samples (n = 11) was compared with Par3 expression in the chronic pancreatitis samples (n = 15). *t* test, mean ± standard deviation (SD); $^{**}P \leq .01$. (*B*) In chronic pancreatitis specimens (n = 15), the relative expression of Par3 in ADM was compared with Par3 expression in the adjacent normal pancreas. *t* test, mean ± SD; $^{**}P \leq .01$. (*C* and *D*) Wild-type B6 mice were treated with 8 hourly injections of cerulein to induce acute pancreatitis (n = 4, 5) or treated with cerulein twice daily for 5 days to induce chronic pancreatitis (n = 4, 4), and the pancreas immunofluorescence stained for Par3 and DAPI. *t* test, mean ± SD; $^{**}P \leq .01$. (*E*) The chronic pancreatitis mouse samples (n = 3) were costained with Par3, CK19, amylase, and DAPI to evaluate Par3 expression in mouse ADM lesions. Par3 expression in the ADM was compared with Par3 expression in the adjacent normal pancreas. In each mouse, at least 10 adjacent regions and ADM lesions were analyzed for Par3 expression. *t* test, mean ± SD; $^{**}P \leq .01$, $^{****}P \leq .0001$. Scale bars in *A*–*E* = 100 mm. IHC, immunohistochemistry; ns, not significant; Ceru, cerulein.

Pancreatic Par3 Loss Exacerbates Acinar Cell Loss in Cerulein-Induced Chronic Pancreatitis

In parallel studies, we evaluated the effects of Par3 loss on acinar cell injury with chronic pancreatitis in 2- to 3-month-old mice (Figure 4*A*). Although both CPar3+/+ and CPar3fl/fl mice lost weight with cerulein treatment, the CPar3fl/fl mice showed a more pronounced weight loss and loss of pancreas weight (Figure 4*B* and *C*). Hematoxylin and eosin staining showed disruption of acinar parenchyma and loss of zymogen granules in the CPar3fl/fl mice after 5 days, loss of acinar cells after 10 days, and a near-total absence of acinar cells after 14 days of cerulein treatment (Figure 4*D*). We also evaluated whether the cerulein-treated CPar3fl/fl mice could recover the pancreas architecture after stopping cerulein treatment. Although the control CPar3+/+ mice quickly regained weight after stopping cerulein treatment, the CPar3fl/fl mice regained weight at a slower rate and failed to fully recover the lost weight 14 days after stopping cerulein treatment (Figure 4*E*). There was also minimal to no recovery of the acinar compartment in the CPar3fl/fl mice 14 days and 2 months after stopping cerulein treatment (Figure 4*F*).

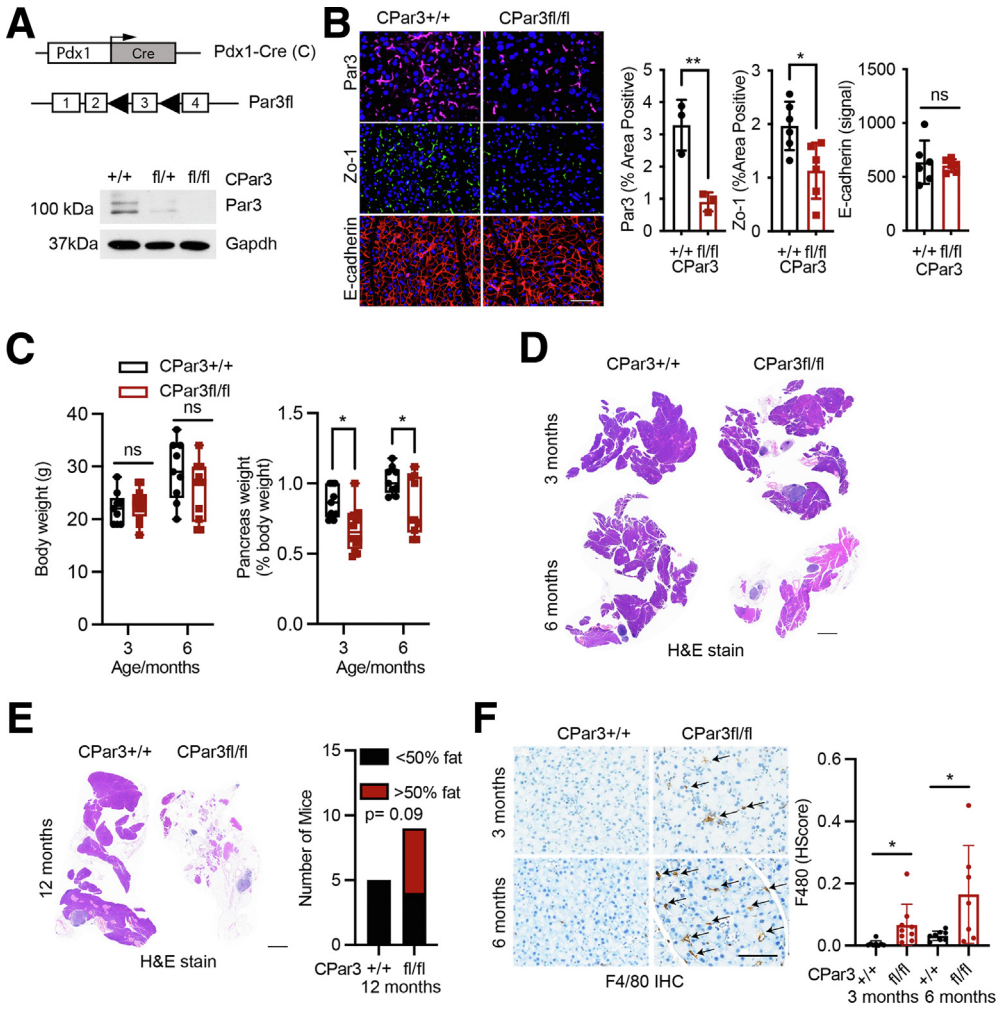

Figure 2. Mice with pancreatic Par3 loss exhibit low-grade inflammation and acinar cell loss with aging. (*A*) Alleles of Pdx1-Cre (*C*) and Par3fl mice. Par3 expression in the pancreas of mice of indicated genotypes was determined by Western blotting. (*B*) Immunofluorescence stains for Par3, Zo-1, and E-cadherin of the pancreas collected from CPar3+/+ and CPar3fl/fl mice at 13 weeks. Scale bar = 50 μm. Quantification of immunofluorescence stains for Par3 (n = 3, 3), Zo-1 (n = 6, 6), and E-cadherin (n = 6, 6). *t* test, mean ± standard deviation (SD); $^{*}P \leq .05$, $^{**}P \leq .01$. (*C*) Body weights and pancreas weights of CPar3+/+ and CPar3fl/fl mice at 3 (n = 9, 10) and 6 (n = 9, 10) months of age. *t* test, mean ± SD; $^{*}P \leq .05$. (*D* and *E*) H&E stains of the pancreas from CPar3+/+ and CPar3fl/fl mice at 3, 6, and 12 months of age. The extent of fat accumulation was assessed as <50% or >50% at 12 months of age (n = 5, 9). Fisher exact test; $P = .09$. Scale bars = 1 mm. (*F*) F4/80 IHC stains of the pancreas from CPar3+/+ and CPar3fl/fl mice at 3 (n = 8, 9) and 6 months (n = 8, 7) of age. *t* test, mean ± SD; $^{*}P \leq .05$. Scale bar = 100 μm. H&E, hematoxylin and eosin; IHC, immunohistochemistry; ns, not significant.

Pancreatic Par3 Loss Exacerbates Fibroinflammatory Reaction in Cerulein-Induced Chronic Pancreatitis

When we examined the effects of Par3 loss on cerulein-induced inflammation (macrophages and neutrophils) in the pancreatitis samples after 5 days of cerulein treatment, we found minimal numbers of neutrophils in the pancreas of CPar3fl/fl mice and CPar3+/+ mice but a significantly increased numbers of macrophages in the pancreas of CPar3fl/fl mice (Figure 5*A*). However, these macrophages did not express increased CD206 levels (M2 reparative macrophages) (Figure 5*A*). Trichrome and α-SMA staining showed that wherever there was preservation of acinar compartment in the pancreas of CPar3fl/fl mice, there was increased fibrosis and activation of myofibroblasts (Figure 5*B*). Thus, following the induction of chronic pancreatitis, the pancreas of CPar3fl/fl mice showed extensive acinar loss with lipomatosis and/or increased fibrosis.

Pancreatic Par3 Loss Results in Reduced Chronic Pancreatitis-Induced ADM and Proliferation

Because ADM is a protective mechanism against tissue damage induced by repeated pancreatic inflammation,[1–5] we stained the chronic pancreatitis specimens from mice treated with cerulein for 5 and 10 days for acinar (amylase)

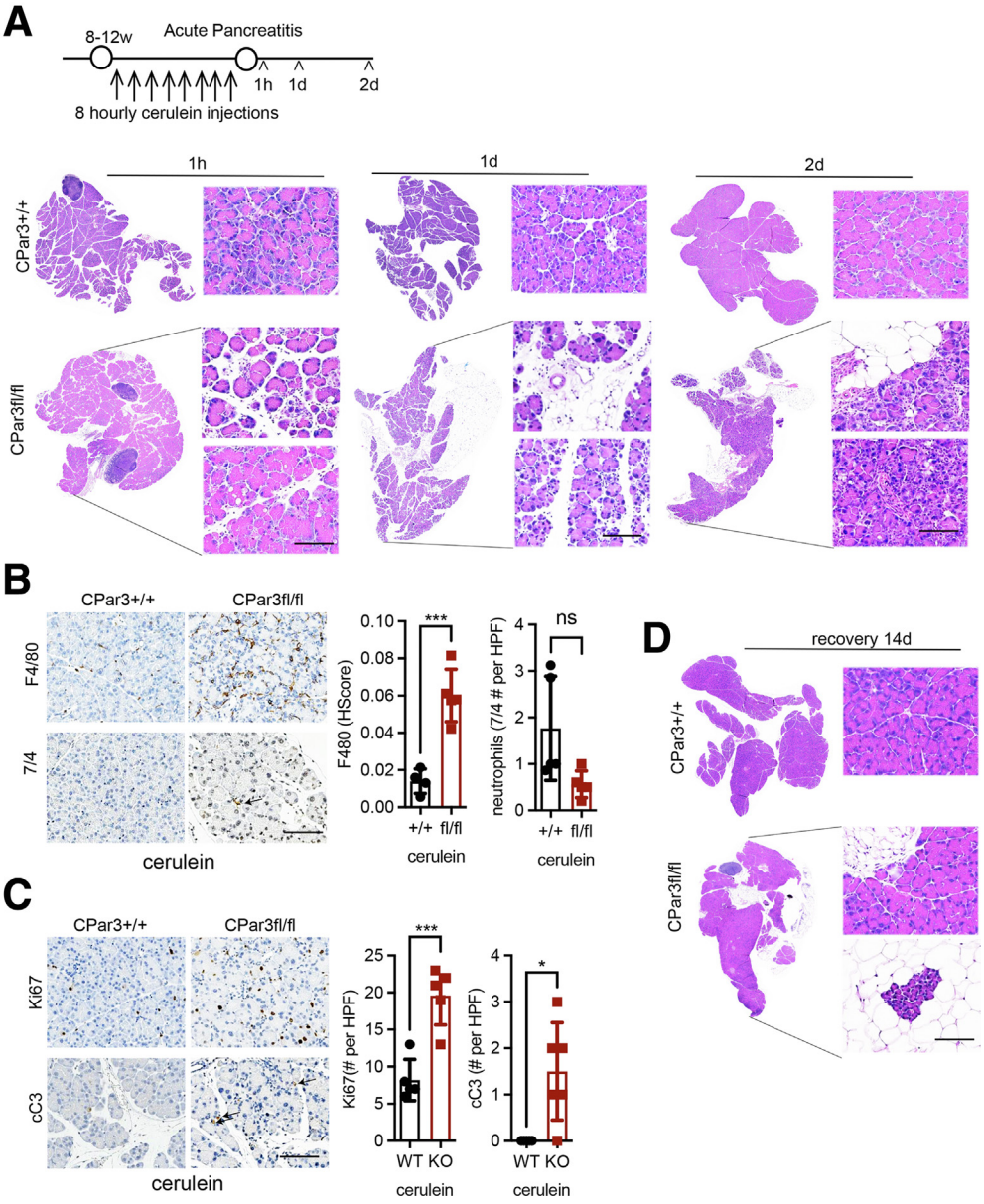

Figure 3. Pancreatic Par3 loss results in exacerbation of cerulein-induced acute pancreatitis. (*A*) CPar3+/+ and CPar3fl/fl mice were treated with 8 hourly intraperitoneal injections of cerulein (50 μg/kg) and the pancreas collected and stained with hematoxylin and eosin 1 hour (n = 5, 5), 1 day (n = 5, 5), or 2 days (n = 5, 5) after the last cerulein injection. (*B* and *C*) The acute pancreatitis specimens collected at 1 day after the last cerulein injection of CPar3+/+ and CPar3fl/fl mice were stained for F4/80 (n = 4, 5), Ly-6B.2, clone 7/4 (n = 5, 5), Ki67 (n = 5, 5), and cC3 (n = 5, 6), and the relative staining was quantified. *t* test, mean ± standard deviation; $^{*}P \leq .05$, $^{***}P \leq .001$. (*D*) The acute pancreatitis specimens collected 14 days after the last cerulein injection of CPar3+/+ and CPar3fl/fl mice were stained with hematoxylin and eosin (n = 4, 4). Scale bars in *A–D* = 100 μm. KO, knock out; ns, not significant; WT, wild-type.

and ductal (CK19) markers. After both 5 and 10 days of cerulein treatment, there was a significant decrease in amylase staining, with decreased costaining of amylase and CK19 in the pancreas of cerulein-treated CPar3fl/fl mice (Figure 6*A* and *C*), indicating that the Par3 loss affects the ability of acinar cells to undergo ADM. When we evaluated the effects of Par3 loss on apoptosis (cC3) and proliferation (Ki67), we found increased cC3 staining after 5 days but not after 10 days of cerulein treatment in the CPar3fl/fl mice (Figure 6*B* and *D*). In contrast, there was a significant reduction in Ki67 staining after both 5 and 10 days of cerulein treatment (Figure 6*B* and *D*). These results suggest that Par3 facilitates chronic pancreatitis-induced ADM, limits chronic pancreatitis-induced acinar injury, and facilitates recovery following acinar injury.

Mice with Pancreatic Par3 Loss Demonstrate Reduced Chronic Pancreatitis-Induced Primary Cilia

To further understand how Par3 loss exacerbates phenotypic changes in our mouse models, we performed RNA sequencing and gene set enrichment analysis of the chronic pancreatitis samples after 5 days of cerulein treatment. The gene set enrichment analysis showed a reduction in the ciliogenesis program in the CPar3fl/fl mice compared with the CPar3+/+ mice (Figure 7*A* and *B*). Importantly, previous reports indicate that loss of pancreatic primary cilia results in pancreatitis and fatty changes.[19,20] When we stained for primary cilia using acetylated tubulin and ADP ribosylation factor like GTPase 13B (Arl13b),[23–25] we found a significant reduction in the acetylated tubulin and Arl13b

in the pancreas of cerulein-treated CPar3fl/fl mice compared with the pancreas of cerulein-treated CPar3+/+ mice (Figure 7*C* and *D*). Furthermore, when we stained the pancreas for FoxJ1, 1 of the key regulators of primary cilia,[26–28] we found that cerulein treatment induced FoxJ1 in the CPar3+/+ mice but the cerulein-treated CPar3fl/fl mice had a near absence of FoxJ1 (Figure 7*E*). These results indicate that mice with pancreatic Par3 loss demonstrate reduced pancreatitis-induced primary cilia. Because ductal cells, but not acinar cells, express primary cilia,[17,29,30] these

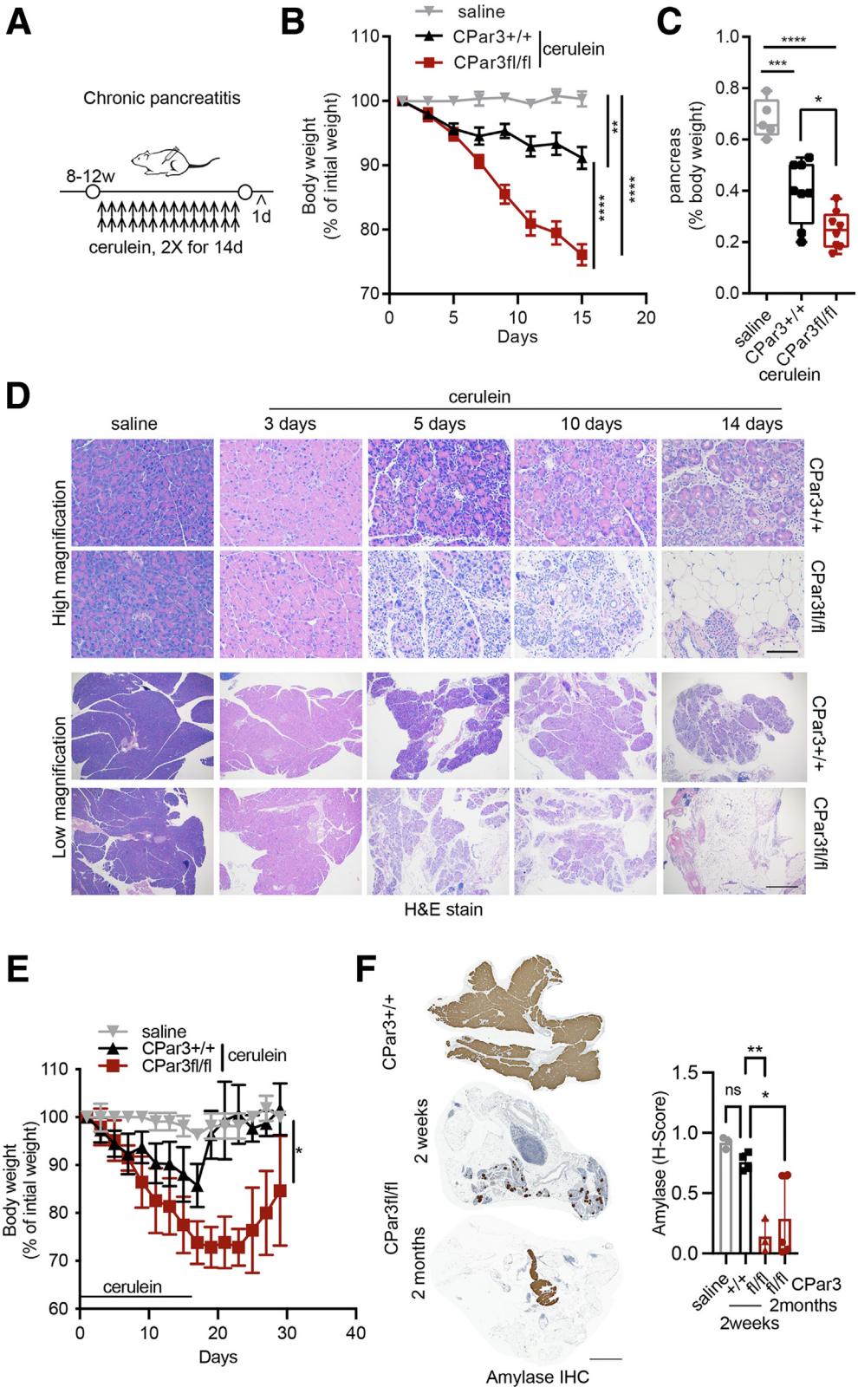

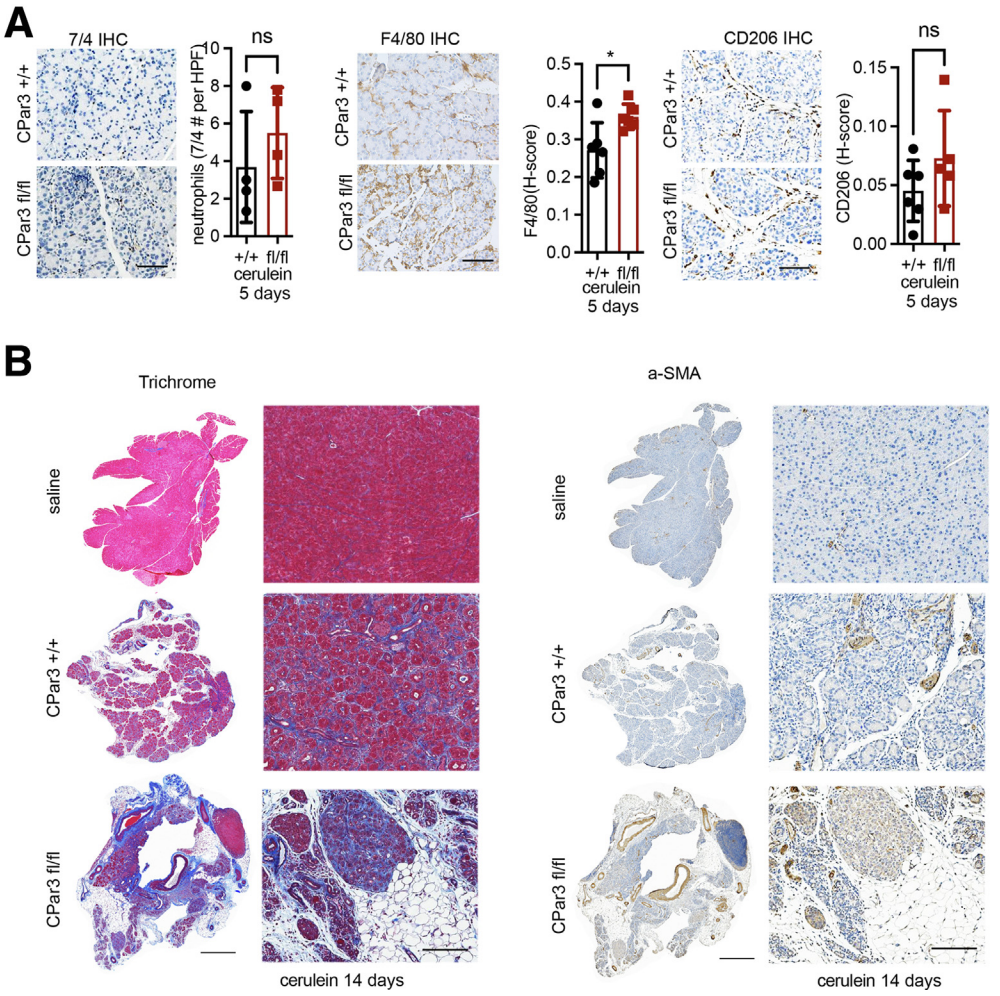

Figure 5. Pancreatitis exacerbates loss of acinar compartment in mice with pancreatic Par3 loss. (*A*) Pancreas from CPar3+/+ and CPar3fl/fl mice treated with cerulein for 5 days were stained for Ly-6B.2, clone 7/4 (n = 4, 4), F4/80 (n = 6, 7), and CD206 (n = 6, 5), and the relative staining was quantified. *t* test, mean ± standard deviation; $^{*}P \leq .05$. Scale bar = 100 μm. (*B*) Pancreas from CPar3+/+ (n = 5) and CPar3fl/fl (n = 5) mice treated with cerulein twice daily for 14 days were trichrome stained or stained for α-SMA. Scale bars for low magnification = 1 mm and scale bars for high magnification = 100 μm. IHC, immunohistochemistry; ns, not significant.

results also support our findings that Par3 loss results in reduced pancreatitis-induced ADM.

Targeting BET Proteins Attenuates Chronic Pancreatitis-Induced Loss of Primary Cilia in Mice Lacking Pancreatic Par3

Because the BET protein Brd4 regulates acinar regeneration following pancreatitis-induced injury,[6] we evaluated the effect of BET inhibition on pancreatitis-induced loss of primary cilia in the CPar3fl/fl mice. The CPar3fl/fl mice were pretreated with the BET inhibitor JQ1 for 1 week and then treated concurrently with JQ1 and cerulein for 5 days (Figure 8*A*). Compared with the control (dimethylsulfoxide) cerulein-treated CPar3fl/fl mice, there was an increase in the ciliogenic program in the CPar3fl/fl mice cotreated with JQ1 and cerulein (Figure 8*A*). Although JQ1 did not attenuate cerulein-induced inflammation (Figure 8*B*), JQ1 enhanced

Figure 4. Pancreatic Par3 loss exacerbates acinar cell loss in cerulein-induced chronic pancreatitis. (*A*) CPar3+/+ and CPar3fl/fl mice were treated with intraperitoneal injections of saline or cerulein (250 μg/kg) twice daily for 14 days. (*B*) Weights of mice treated with saline (n = 8) or cerulein (CPar3+/+, n = 12; CPar3fl/fl, n = 11) during treatment. One-way analysis of variance at end of treatment, mean ± standard deviation (SD); $^{**}P \leq .01$, $^{****}P \leq .0001$. (*C*) Pancreas weights as a percentage of body weight were determined for mice treated with saline (n = 5) or cerulein (CPar3+/+, n = 8; CPar3fl/fl, n = 8). One-way analysis of variance, mean ± min to max; $^{*}P \leq .05$, $^{***}P \leq .001$, $^{****}P \leq .0001$. (*D*) CPar3+/+ and CPar3fl/fl mice were treated with cerulein (250 μg/kg) twice daily for 3 days (n = 6, 5), 5 days (n = 7, 7), 10 days (n = 3, 6), and 14 (n = 4, 5) days and the pancreas hematoxylin and eosin stained. (*E*) CPar3+/+ and CPar3fl/fl mice were treated with saline or cerulein (250 μg/kg) twice daily for 14 days. Weights of mice treated with saline (n = 4) or cerulein (CPar3+/+, n = 7; CPar3fl/fl, n = 9) during and after treatment. *t* test, mean ± SD; $^{*}P \leq .05$. (*F*) Amylase staining of the pancreas 2 weeks (saline, n = 3; cerulein, CPar3+/+, n = 4; cerulein, CPar3fl/fl, n = 3) and 2 months (cerulein, CPar3fl/fl, n = 5) postcerulein treatment, and the relative amylase staining was quantified. One-way analysis of variance, mean ± SD; $^{*}P \leq .05$, $^{**}P \leq .01$. Scale bars for low magnification in *D* and *F* = 1 mm. Scale bars for high magnification in *D* = 100 μm. H&E, hematoxylin and eosin; IHC, immunohistochemistry; ns, not significant.

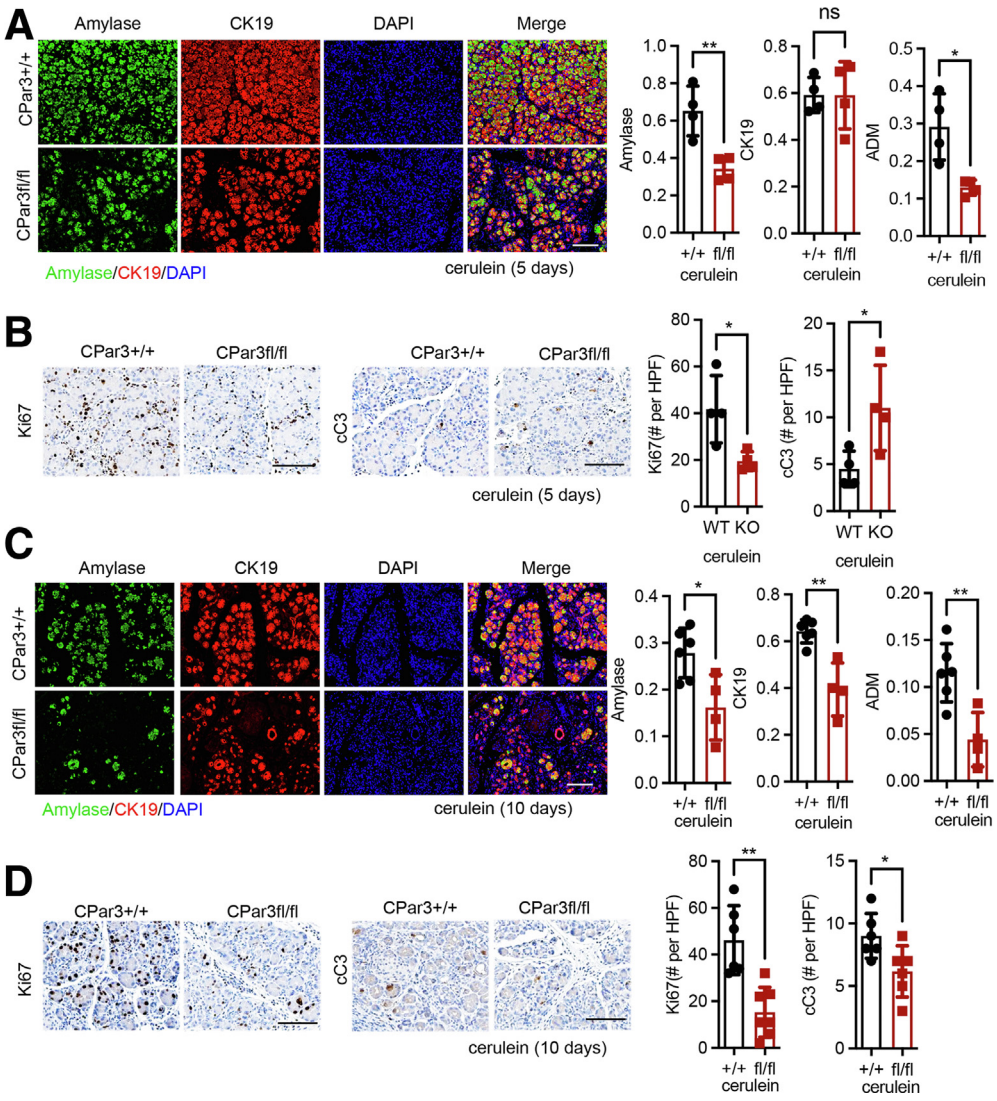

Figure 6. Par3 loss results in reduced chronic pancreatitis-induced ADM formation and proliferation. CPar3+/+ and CPar3fl/fl mice were treated with intraperitoneal injections of cerulein (250 μg/kg) twice daily for 5 or 10 days. (*A* and *C*) The chronic pancreatitis mouse samples were costained with amylase, CK19, and DAPI to evaluate mouse ADM lesions, and the relative staining was quantified. (n = 4, 4 for samples in *A*; n = 6, 4 for samples in *C*). *t* test, mean ± standard deviation; $^{*}P \leq .05$, $^{**}P \leq .01$. Scale bar = 100 μm. (*B* and *D*) The specimens were stained for Ki67 and cC3, and the relative staining was quantified. (n = 4, 4 for samples in *B*; n = 6, 7 for samples in *D*). *t* test, mean ± standard deviation; $^{*}P \leq .05$; $^{**}P \leq .01$. Scale bar = 100 μm. KO, knock out; ns, not significant; WT, wild-type.

the expression of FoxJ1, acetylated tubulin, and Arl13b in the cerulein-treated CPar3fl/fl mice (Figure 8*C*–*E*). These results indicate that targeting BET proteins mitigates the effects of Par3 loss on pancreatitis-induced primary ciliogenesis.

Targeting BET Proteins Promotes ADM in Mice Lacking Pancreatic Par3

In additional studies, we evaluated the effects of JQ1 on amylase, CK-19, and ADM by costaining for CK-19 and amylase. JQ1 enhanced amylase expression without affecting the levels of CK19 in the cerulein-treated CPar3fl/fl mice (Figure 9*A*). JQ1 also almost doubled the extent of ADM in the cerulein-treated CPar3fl/fl mice, with the increased ADM trending towards statistical significance (Figure 9*A*). JQ1 increased proliferation (Ki67) in the cerulein-treated CPar3fl/fl mice but did not suppress apoptosis (cC3) (Figure 9*B*). These results indicate that targeting BET proteins mitigates the effects of Par3 loss on chronic pancreatitis-induced ADM and facilitates recovery following acinar injury in mice with Par3 loss.

Targeting BET Proteins Attenuates Cerulein-Induced Acinar Cell Loss in Mice Lacking Pancreatic Par3 and Enhance Recovery of Acinar Cell Mass and Body Weight

Finally, we evaluated the effects of BET inhibitors on cerulein-induced acinar cell loss in the CPar3fl/fl and the CPar3+/+ mice. JQ1 did not prevent weight loss in cerulein-treated CPar3+/+ and CPar3fl/fl mice (Figure 10*A*). However, histologic examination showed preservation of the acinar compartment in the CPar3fl/fl mice, as demonstrated by amylase staining (Figure 10*B*). Consequently, pretreatment with JQ1 accelerated the recovery of body mass of both CPar3+/+ and CPar3fl/fl mice (Figure 10*C*). Histologic examination showed significant recovery of the acinar compartment of CPar3fl/fl mice, as demonstrated by amylase staining (Figure 10*D*).

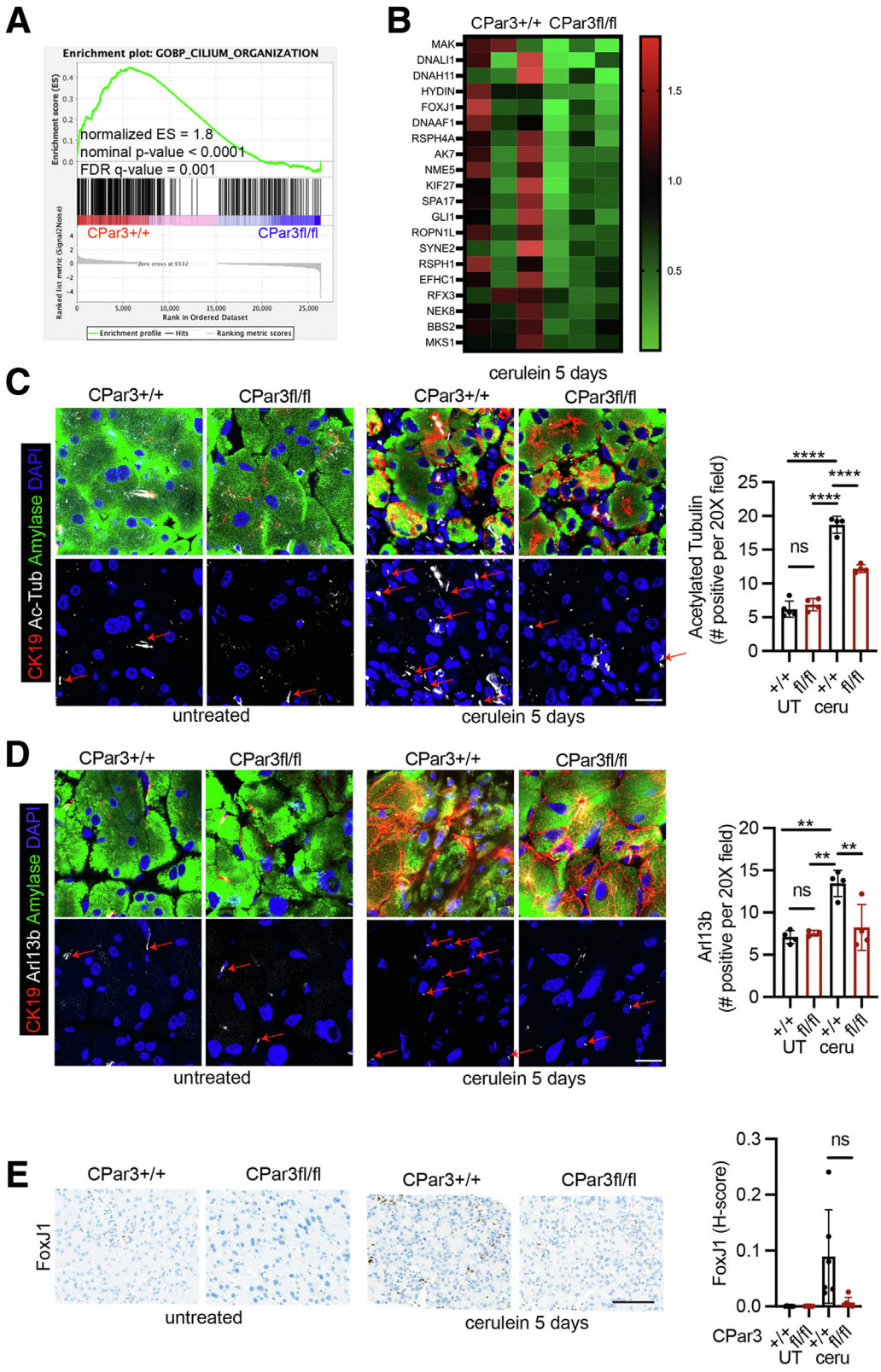

Figure 7. Mice with pancreatic Par3 loss demonstrate reduced chronic pancreatitis-induced primary cilia. (*A* and *B*) CPar3+/+ and CPar3fl/fl mice were treated with intraperitoneal injections of cerulein (250 μg/kg) twice daily for 5 days. Gene set enrichment analysis and enrichment plot for primary cilium using Day 5 pancreatitis RNA samples from CPar3+/+ and CPar3fl/fl mice (n = 3, 3). Heatmap for the top genes associated with the primary cilium. (*C–E*) Pancreas from control (UT) CPar3+/+ and CPar3fl/fl mice or from mice treated with cerulein for 5 days were stained for acetylated tubulin (n = 5, 4, 4, 4), Arl13b (n = 4, 3, 4, 4), and FoxJ1 (n = 5, 5, 5, 5), and the relative staining was quantified. One-way analysis of variance, mean ± standard deviation; $^{**}P \leq .01$, $^{****}P \leq .0001$. Scale bar in *C* and *D* = 25 μm and in *E* =100 μm. ns, not significant; UT, untreated.

Discussion

The polarity proteins have been studied extensively in tumorigenesis[31,32]; however, their role in normal tissue homeostasis has yet to be fully understood. For example, loss of Par3 in the prostate tissue promotes proliferation and causes high-grade prostatic intraepithelial neoplastic lesions.[33]

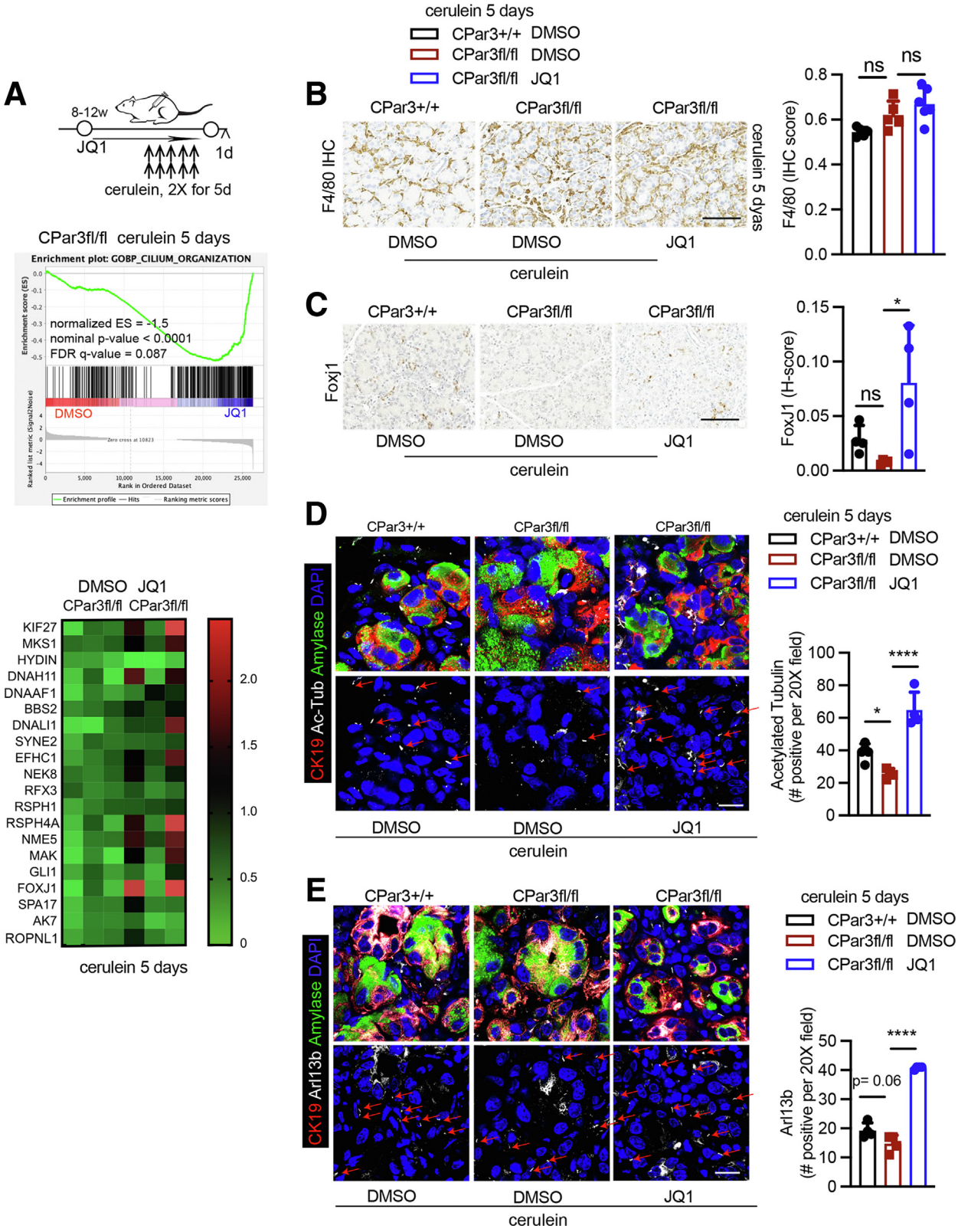

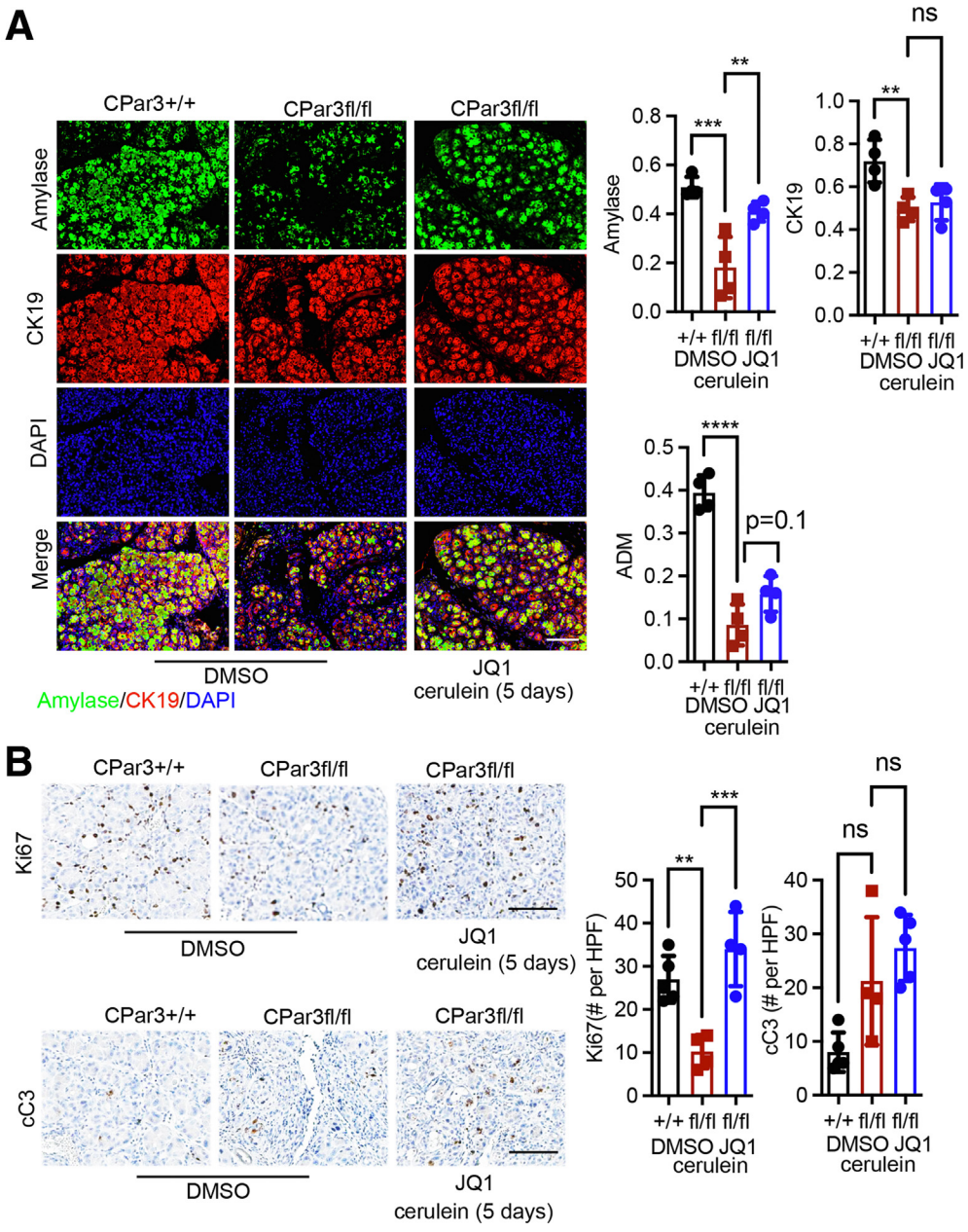

Figure 9. BET inhibition promotes ADM in mice lacking pancreatic Par3. CPar3+/+ and CPar3fl/fl mice were treated with DMSO or JQ1 (50 mg/kg) for 7 days and then concurrently treated with DMSO or JQ1 (50 mg/kg) and cerulein (250 μg/kg) for additional 5 days. (*A*) The chronic pancreatitis mouse samples were costained with amylase, CK19, and DAPI to evaluate mouse ADM lesions, and the relative staining was quantified. (n = 4, 4, 4). One-way analysis of variance, mean ± standard deviation; $^{**}P \leq .01$, $^{***}P \leq .001$, $^{****}P \leq .0001$. Scale bar = 100 μm. (*B*) The specimens were stained for Ki67 and cC3, and the relative staining was quantified. (n = 5, 4, 4). *t* test, mean ± standard deviation; $^{**}P \leq .01$, $^{***}P \leq .001$. Scale bar = 100 μm. DMSO, dimethylsulfoxide; ns, not significant.

Similarly, the loss of Par3 in the epidermis causes aberrant proliferation and differentiation.[21] Moreover, targeting Par3 in mouse mammary progenitor cells causes ductal hyperplasia and disorganized end bud structures that fail to remodel into typical ductal structures when transplanted.[34] In contrast to these studies, we show that loss of Par3 in the pancreas does not

Figure 8. (***See previous page***). **BET inhibition attenuates pancreatitis-induced loss of primary cilia in mice lacking pancreatic Par3.** (*A*) CPar3+/+ and CPar3fl/fl mice were treated with DMSO or JQ1 (50 mg/kg) for 7 days and then concurrently treated with DMSO or JQ1 (50 mg/kg) and cerulein (250 μg/kg) for additional 5 days. Gene set enrichment analysis and enrichment plot for primary cilium using RNA samples from CPar3fl/fl mice treated with cerulein and cotreated with DMSO or JQ1 (n = 3, 3). Heatmap for the top genes associated with the primary cilium. (*B*) CPar3+/+ and CPar3fl/fl mice were treated with DMSO or JQ1 (50 mg/kg) for 7 days and then concurrently treated with DMSO or JQ1 (50 mg/kg) and cerulein (250 μg/kg) for additional 5 days. Pancreas were stained for F4/80 (n = 5, 5, 6), and the relative staining was quantified. One-way analysis of variance, mean ± standard deviation. Scale bar = 100 μm. (*C–E*) Pancreatic sections from mice treated with cerulein for 5 days and cotreated with DMSO or JQ1 were stained for FoxJ1 (n = 4, 4, 5), acetylated tubulin (n = 5, 4, 4), and Arl13b (n = 4, 4, 4) and the relative staining was quantified. One-way analysis of variance, mean ± standard deviation; $^{*}P \leq .05$, $^{****}P \leq .0001$, Scale bar in *C* = 100 μm and in *D* and *E* = 25 μm. DMSO, dimethylsulfoxide; ns, not significant.

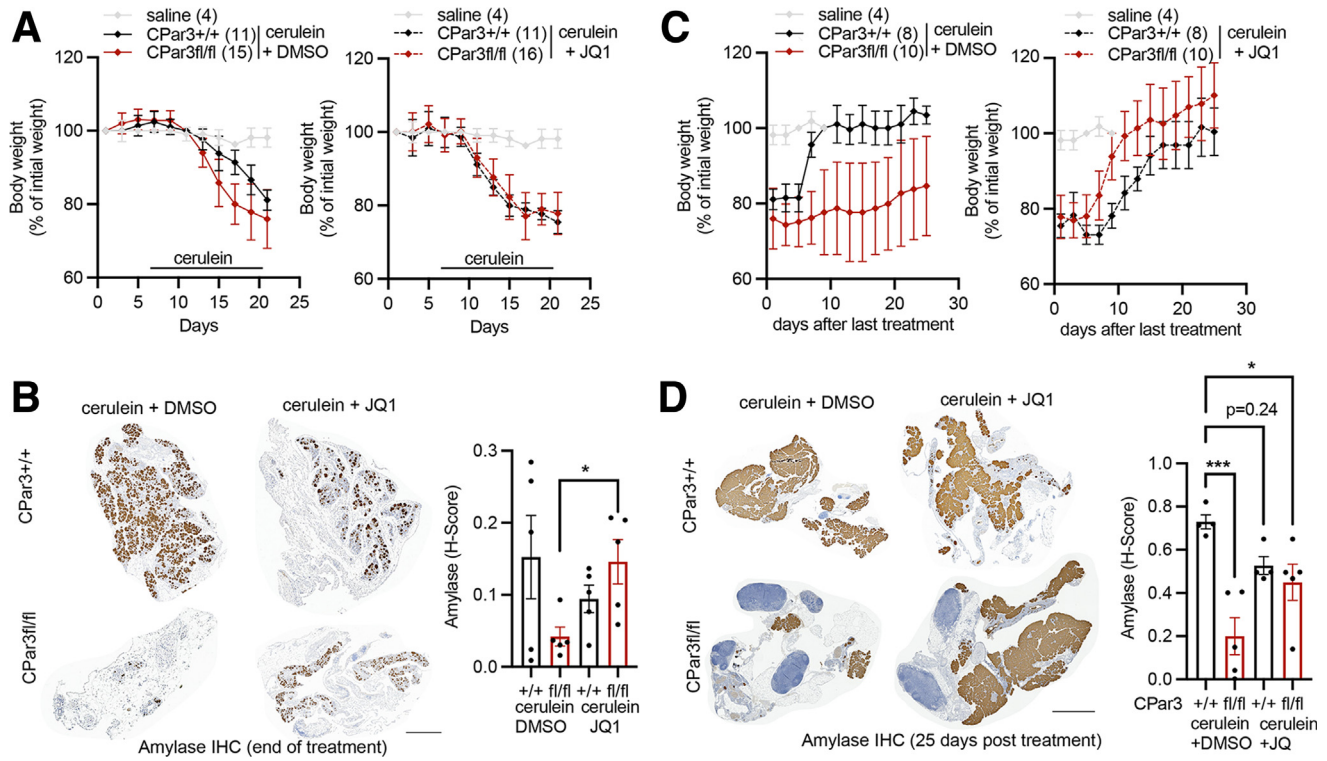

Figure 10. BET inhibitors attenuate cerulein-induced acinar cell loss in mice lacking pancreatic Par3 and enhance recovery of acinar cell mass and body weight. (*A* and *B*) CPar3+/+ and CPar3fl/fl mice were treated with DMSO or JQ1 (50 mg/kg) for 7 days and then concurrently treated with DMSO or JQ1 (50 mg/kg) and cerulein (250 μg/kg) for additional 2 weeks. Mice were monitored for weight loss during treatment. Acinar cell loss at the end of treatment was analyzed by amylase staining (n = 5, 5, 5, 5), and the relative amylase staining was quantified. One-way analysis of variance, mean ± standard deviation. *$P \leq .05$. Scale bar = 1 mm. (*C* and *D*) CPar3+/+ and CPar3fl/fl were pretreated with DMSO or JQ1 (50 mg/kg) for 7 days and then concurrently treated with DMSO or JQ1 (50 mg/kg) and cerulein (250 μg/kg) for 2 weeks. Mice were then monitored for additional 25 days. Recovery of body weights monitored over 25 days. Acinar cell recovery 25 days post-treatment was analyzed by amylase staining (n = 4, 5, 4, 5), and the relative amylase staining was quantified. One-way analysis of variance, mean ± standard deviation; *$P \leq .05$, ***$P \leq .001$. Scale bar = 1 mm. DMSO, dimethylsulfoxide; IHC, immunohistochemistry.

affect pancreas development and results in reduced proliferation with induction of chronic pancreatitis.

However, one of the most dramatic phenotypes in mice with pancreatic Par3 loss is the extensive loss of the acinar compartment with aging and following induction of chronic pancreatitis. We show increased apoptosis early in chronic pancreatitis-induced tissue injury. Loss of epidermal Par3 is also associated with increased apoptosis following treatment with DMBA/TPA.[35] Par3 in the epidermis maintains mitotic accuracy and cellular fitness by integrating biomechanical signaling and cell division.[22] These results suggest that the disruption of apical-basal polarity induces apoptosis, possibly as a protective mechanism against transformation in damaged tissue. We also show that in mice with pancreatic Par3 loss, there is increased inflammation following the induction of pancreatitis and with aging. Notably, mice lacking Par3 in the endothelium demonstrate increased macrophage infiltration in the aortic arch,[36] indicating that Par3 limits endothelial inflammation in blood vessels under laminar flow.[36] These results suggest that Par3 restrains tissue injury and inflammation in multiple organ systems to maintain tissue homeostasis.

We found that mice with pancreatic Par3 loss exhibit reduced ability to undergo pancreatitis-induced ADM. ADM is a protective mechanism against tissue damage induced by repeated pancreatic inflammation by decreasing zymogen production and secretion.[1–5] Importantly, we show increased Par3 expression in ADM lesions in human and mouse chronic pancreatitis specimens. ADM also facilitates acinar pancreas regeneration after the resolution of the inflammatory stimulus.[1–5] Thus, the failure to undergo ADM can result in acinar damage and delay or prevent acinar regeneration. Also, in contrast to the acinar cells, the ductal cells express primary cilia,[17,29,30] contributing to pancreas regeneration. We show that mice with Par3 loss fail to generate primary cilia following induction of chronic pancreatitis and develop pronounced acinar cell loss and lipomatosis. Notably, a lack of primary cilia in the pancreas results in severe pancreatic abnormalities, including acinar cell loss and associated lipomatosis.[19,20] Our findings agree with a recent study showing that loss of Par3 in neural precursors perturbs the integrity of primary cilia.[37] Also, an earlier study showed that Par3 is required for the development of primary cilia in MDCK cells.[38]

We show that mice with Par3 loss demonstrate minimal to no recovery of the acinar compartment following induction of pancreatitis. However, targeting BET proteins attenuates cerulein-induced acinar cell loss and enhances acinar cell mass recovery in these mice. The Scott Lowe laboratory had previously shown that genetic targeting of Brd4 using shRNA enhanced pancreatitis-induced acinar injury but prevented subsequent regeneration.[6] We have also found that targeting BET proteins with the BET inhibitor JQ1 exacerbated pancreatitis-induced injury in control mice. However, in mice with Par3 loss, although JQ1 did not attenuate pancreatitis-induced inflammation, JQ1 enhanced ADM formation and attenuated pancreatitis-induced acinar cell loss. Also, when we stopped JQ1 treatment, in contrast to the irreversible knockdown of Brd4 with shRNA,[6] we found that both the control mice and mice with pancreatic Par3 loss demonstrated recovery of acinar cell mass and body weight. Unexpectedly, we found that JQ1 rescued chronic pancreatitis-induced primary cilia in mice with Par3 loss. Interestingly, several small molecule inhibitors induce ciliogenesis by modulating Aurora-A (AURKA) activity,[39,40] one of the central regulators of ciliary disassembly.[41,42] In future studies, we will evaluate how BET inhibitors promote primary cilia.

Overall, our study increases the understanding of the role of the polarity protein Par3 in pancreatitis and paves the way for potential therapeutic intervention. We identify BET inhibitors as a possible strategy to attenuate pancreas injury and facilitate regeneration.

Methods

Animal Experiments

Conditional Knockout. Mice with loss of Par3 in the pancreas were generated by crossing Pdx1-Cre mice (Jackson Laboratory #014647) to mice expressing the floxed allele of *Par3*,[43,44] to generate C•Par3fl/+ and C•Par3fl/fl mice. All mice were bred on a C57/BL6 background, and both genders were used in the studies. The studies conform to the Animal Research: Reporting of In Vivo Experiments (ARRIVE) guidelines.

Induction of Pancreatitis. Pancreatitis was induced in age- and litter-matched 8- to 12-week-old mice of both genders. For acute pancreatitis, mice were starved of food overnight, followed by 8 hourly intraperitoneal injections of cerulein (50 μg/kg). Chronic pancreatitis was induced by intraperitoneal injections of cerulein (250 μg/kg) 2 times daily for 3, 5, 10, and 14 days, and the pancreas was collected 16–20 hours later. In additional studies, mice were treated with the BET inhibitor JQ1 (50 mg/kg[45–47]) once daily for 1 week and then treated concurrently with JQ1 once daily and cerulein 2 times daily for 5 days.

Human Pancreatitis Samples

Formalin-fixed paraffin-embedded tissue arrays containing human pancreatitis samples were obtained from US Biomax (PA691). The array panel has 68 cores with 4 acute, 7 mild, and 57 chronic pancreatitis cases.

Histology/Immunohistochemistry

For immunostains, paraffin-embedded sections were deparaffinized and rehydrated. Antigen retrieval was performed by boiling for 10 minutes in either Tris EDTA (10 mM Tris 1 mM EDTA, 0.05% Tween 20, pH 9.0) or sodium citrate buffer (10 mM sodium citrate, 0.05% Tween 20, pH 6.0) using a pressure cooker. Endogenous peroxidase activity in tissue was quenched, and sections were blocked with a mixture of goat serum and bovine serum albumin. Tissue sections were incubated with primary antibodies: F4/80 (Cell Signaling #70076, 1:800), Ly-6B.2, clone 7/4 (BioRad #MCA771GT, 1:1000), cleaved caspase-3 (Cell Signaling Cat #9664, 1:1000), Ki67 (Abcam #Ab15580, 1:1000), Amylase (Cell Signaling #3796, 1:2000), Par3 (Millipore-Sigma #HPA030443, 1:400), and FoxJ1 (Abcam #ab235445, 1:500) overnight at 4^{o}C. Antibody binding was detected using horseradish peroxidase–conjugated anti-rabbit secondary antibody (Vector Laboratories, MP-7451) and visualized using ImmPACT DAB Peroxidase Substrate kit (Vector Laboratories, SK-4105). Photographs were taken on the TissueGnostics system and analyzed by ImageJ or Aperio Software (Leica Biosystems). Hematoxylin and eosin and alcian blue stains were performed by the Northwestern University Pathology Core Facility.

Immunofluorescence

In select experiments, freshly isolated tissue samples were snap-frozen in optimal cutting temperature (OCT) compund, and then sections were fixed in cold acetone:-methanol (1:1) for 20 minutes. After antigen retrieval (similar to immunohistochemistry), tissue sections were stained using the mouse-on-mouse immunodetection kit (Vector Laboratories, BMK-2202). Tissue sections were blocked with mouse-on-mouse blocking reagent for 1 hour at room temperature, followed by washing and incubation with mouse-on-mouse diluent for 5 minutes. Tissue sections were then incubated with primary antibodies: Par3 (Millipore Sigma #07-330, 1:100), E-cadherin (BD Biosciences #610181, 1:500), Zo-1 (Santa Cruz Biotech #sc-33725, 1:200), Amylase (Santa Cruz Biotech #sc-46657, 1:500), CK19 (Developmental Studies Hybridoma Bank TROMAIII, 1:100), acetylated tubulin (acetyl K40) (Abcam #ab179484, 1:1000), and Arl13b (Developmental Studies Hybridoma Bank N295B/66 1:10) for 1 hour at room temperature or at 4^{o}C overnight. After washing, the sections were incubated with Alexa Fluor conjugated secondary antibodies (Thermo Fisher goat anti-rabbit AF488 Plus #A32731, goat anti-mouse AF647 #A21235, and goat anti-rat AF546 #A11081) for 30 minutes in the dark at room temperature. The tissue sections were washed and incubated with DAPI (Thermo Fisher D1306) for 10 minutes. Slides were mounted with fluorescence mounting media and images acquired using the EVOS M5000 epifluorescence microscope (Thermo Fisher). Images were also acquired using the Nikon A1 confocal laser scanning microscope equipped with 4 laser lines (405, 488, 561) and high sensitivity GaAsP detectors.

Western Blot

Tissue samples were finely ground and lysed with cold RIPA lysis buffer containing protease and phosphatase inhibitors. The lysates were then clarified by centrifugation at 10,000 rpm for 10 minutes at 4°C, and the protein concentration was determined using Precision Red solution (Cytoskeleton, Inc, Denver, CO). Equal amounts of protein were separated with a 10% sodium dodecyl-sulfate polyacrylamide gel electrophoresis. The separated proteins were transferred to a nitrocellulose membrane using the semidry transfer system (Bio-Rad). After blocking for 1 hour at room temperature with 5% bovine serum albumin, the membranes were incubated overnight at 4°C with primary antibodies. Primary antibodies used include Par3 (Millipore Sigma #07-330, 1:1000) and GAPDH (Millipore Sigma #MAB374, 1:5000). Horseradish peroxidase–conjugated rabbit (A6667) or mouse (A4416) secondary antibody (Millipore-Sigma, St. Louis, MO) was used with SuperSignal West Pico PLUS (Thermo Fisher Scientific) for protein detection.

RNAseq

RNA was extracted from mouse pancreas tissue using the RNeasy kit. The RNA was submitted to Active Motif, Inc (Carlsbad, CA) for cDNA library preparation and sequencing. The FASTQ and BAM files along with analyses including differential analysis (DESeq2 software) and gene set enrichment analysis (MSigDB C5 GO gene set) results were provided. The raw FASTQ and processed files were deposited in the Gene Expression Omnibus with accession number GSE243623.

Polymerase Chain Reaction

Genomic DNA was isolated from mouse tail biopsies using the GenElute Mammalian Genomic DNA extraction kit (Millipore-Sigma, G1N350-1KT) according to the manufacturer's instructions. The REDTaq ReadyMix polymerase chain reaction mix was use to amplify specific DNA fragments using primers for Pdx1-Cre (forward: CCT GGA AAA TGC TTC TGT CCG; and reverse: CAG GGT GTT ATA AGC AAT CCC) and Par3fl (forward: AGG CTA GCC TGG GTG ATT TGA GAC C; and reverse: TTC CCT GAG GCC TGA CAC TCC AGT C). The amplified DNA was resolved on an agarose gel and imaged using the ChemiDOC system (Bio-Rad).

Statistics

Statistical details of experiments can be found in the figure legends, including the statistical tests used and the number of animals. All statistical analyses were done using GraphPad Prism. The in vivo and in vitro results were compared using 1-way analysis of variance with Tukey correction or 2-tailed t test analysis. Error bars represent standard deviation as specified in the figure legends. A $P < .05$ was considered significant.

Study Approval

The Northwestern University Institutional Animal Care and Use Committee approved all animal work and procedures. The animal experiments were performed per relevant guidelines and regulations. The animals were housed at 12-hour light/dark cycle in ventilated cages with controlled temperature and humidity. The animals were provided water and a standard mouse diet ad libitum, with bedding changed regularly.

References

1. Murtaugh LC, Keefe MD. Regeneration and repair of the exocrine pancreas. Annu Rev Physiol 2015;77:229–249.
2. Zhou Q, Melton DA. Pancreas regeneration. Nature 2018; 557:351–358.
3. Giroux V, Rustgi AK. Metaplasia: tissue injury adaptation and a precursor to the dysplasia-cancer sequence. Nat Rev Cancer 2017;17:594–604.
4. Storz P. Acinar cell plasticity and development of pancreatic ductal adenocarcinoma. Nat Rev Gastroenterol Hepatol 2017;14:296–304.
5. Del Poggetto E, Ho IL, Balestrieri C, et al. Epithelial memory of inflammation limits tissue damage while promoting pancreatic tumorigenesis. Science 2021;373: eabj0486.
6. Alonso-Curbelo D, Ho YJ, Burdziak C, et al. A gene-environment-induced epigenetic program initiates tumorigenesis. Nature 2021;590:642–648.
7. Wauters E, Sanchez-Arevalo Lobo VJ, Pinho AV, et al. Sirtuin-1 regulates acinar-to-ductal metaplasia and supports cancer cell viability in pancreatic cancer. Cancer Res 2013;73:2357–2367.
8. Sahai V, Redig AJ, Collier KA, et al. Targeting BET bromodomain proteins in solid tumors. Oncotarget 2016; 7:53997–54009.
9. Stathis A, Bertoni F. BET proteins as targets for anticancer treatment. Cancer Discov 2018;8:24–36.
10. Grimont A, Leach SD, Chandwani R. Uncertain beginnings: acinar and ductal cell plasticity in the development of pancreatic cancer. Cell Mol Gastroenterol Hepatol 2022;13:369–382.
11. Guzman-Herrera A, Mao Y. Polarity during tissue repair, a multiscale problem. Curr Opin Cell Biol 2020;62:31–36.
12. Riga A, Castiglioni VG, Boxem M. New insights into apical-basal polarization in epithelia. Curr Opin Cell Biol 2020;62:1–8.
13. Chen J, Zhang M. The Par3/Par6/aPKC complex and epithelial cell polarity. Exp Cell Res 2013; 319:1357–1364.
14. Martin-Belmonte F, Mostov K. Regulation of cell polarity during epithelial morphogenesis. Curr Opin Cell Biol 2008;20:227–234.
15. Thompson BJ. Par-3 family proteins in cell polarity & adhesion. FEBS J 2022;289:596–613.
16. Anvarian Z, Mykytyn K, Mukhopadhyay S, et al. Cellular signalling by primary cilia in development, organ function and disease. Nat Rev Nephrol 2019;15:199–219.
17. Lodh S, O'Hare EA, Zaghloul NA. Primary cilia in pancreatic development and disease. Birth Defects Res C Embryo Today 2014;102:139–158.
18. Silva DF, Cavadas C. Primary cilia shape hallmarks of health and aging. Trends Mol Med 2023;29:567–579.

19. Cano DA, Sekine S, Hebrok M. Primary cilia deletion in pancreatic epithelial cells results in cyst formation and pancreatitis. Gastroenterology 2006;131:1856–1869.
20. Augereau C, Collet L, Vargiu P, et al. Chronic pancreatitis and lipomatosis are associated with defective function of ciliary genes in pancreatic ductal cells. Hum Mol Genet 2016;25:5017–5026.
21. Ali NJA, Dias Gomes M, Bauer R, et al. Essential role of polarity protein Par3 for epidermal homeostasis through regulation of barrier function, keratinocyte differentiation, and stem cell maintenance. J Invest Dermatol 2016; 136:2406–2416.
22. Dias Gomes M, Letzian S, Saynisch M, et al. Polarity signaling ensures epidermal homeostasis by coupling cellular mechanics and genomic integrity. Nat Commun 2019;10:3362.
23. Piperno G, Fuller MT. Monoclonal antibodies specific for an acetylated form of alpha-tubulin recognize the antigen in cilia and flagella from a variety of organisms. J Cell Biol 1985;101:2085–2094.
24. Larkins CE, Aviles GD, East MP, et al. Arl13b regulates ciliogenesis and the dynamic localization of Shh signaling proteins. Mol Biol Cell 2011;22:4694–4703.
25. Cantagrel V, Silhavy JL, Bielas SL, et al. Mutations in the cilia gene ARL13B lead to the classical form of Joubert syndrome. Am J Hum Genet 2008;83:170–179.
26. Yu X, Ng CP, Habacher H, et al. Foxj1 transcription factors are master regulators of the motile ciliogenic program. Nat Genet 2008;40:1445–1453.
27. Thomas J, Morle L, Soulavie F, et al. Transcriptional control of genes involved in ciliogenesis: a first step in making cilia. Biol Cell 2010;102:499–513.
28. Choksi SP, Lauter G, Swoboda P, et al. Switching on cilia: transcriptional networks regulating ciliogenesis. Development 2014;141:1427–1441.
29. Cano DA, Murcia NS, Pazour GJ, et al. Orpk mouse model of polycystic kidney disease reveals essential role of primary cilia in pancreatic tissue organization. Development 2004;131:3457–3467.
30. Ait-Lounis A, Baas D, Barras E, et al. Novel function of the ciliogenic transcription factor RFX3 in development of the endocrine pancreas. Diabetes 2007;56:950–959.
31. Fomicheva M, Tross EM, Macara IG. Polarity proteins in oncogenesis. Curr Opin Cell Biol 2020;62:26–30.
32. Muthuswamy SK, Xue B. Cell polarity as a regulator of cancer cell behavior plasticity. Annu Rev Cell Dev Biol 2012;28:599–625.
33. Zhou PJ, Wang X, An N, et al. Loss of Par3 promotes prostatic tumorigenesis by enhancing cell growth and changing cell division modes. Oncogene 2019; 38:2192–2205.
34. McCaffrey LM, Macara IG. The Par3/aPKC interaction is essential for end bud remodeling and progenitor differentiation during mammary gland morphogenesis. Genes Dev 2009;23:1450–1460.
35. Vorhagen S, Kleefisch D, Persa OD, et al. Shared and independent functions of aPKClambda and Par3 in skin tumorigenesis. Oncogene 2018;37:5136–5146.
36. Hikita T, Mirzapourshafiyi F, Barbacena P, et al. PAR-3 controls endothelial planar polarity and vascular inflammation under laminar flow. EMBO Rep 2018;19:e45253.
37. Hirose T, Sugitani Y, Kurihara H, et al. PAR3 restricts the expansion of neural precursor cells by regulating hedgehog signaling. Development 2022;149:dev199931.
38. Sfakianos J, Togawa A, Maday S, et al. Par3 functions in the biogenesis of the primary cilium in polarized epithelial cells. J Cell Biol 2007;179:1133–1140.
39. Kiseleva AA, Korobeynikov VA, Nikonova AS, et al. Unexpected activities in regulating ciliation contribute to off-target effects of targeted drugs. Clin Cancer Res 2019;25:4179–4193.
40. Khan NA, Willemarck N, Talebi A, et al. Identification of drugs that restore primary cilium expression in cancer cells. Oncotarget 2016;7:9975–9992.
41. Pugacheva EN, Jablonski SA, Hartman TR, et al. HEF1-dependent Aurora A activation induces disassembly of the primary cilium. Cell 2007;129:1351–1363.
42. Kobayashi T, Itoh H. Loss of a primary cilium in PDAC. Cell Cycle 2017;16:817–818.
43. Iden S, van Riel WE, Schafer R, et al. Tumor type-dependent function of the par3 polarity protein in skin tumorigenesis. Cancer Cell 2012;22:389–403.
44. Hirose T, Karasawa M, Sugitani Y, et al. PAR3 is essential for cyst-mediated epicardial development by establishing apical cortical domains. Development 2006; 133:1389–1398.
45. Delmore JE, Issa GC, Lemieux ME, et al. BET bromodomain inhibition as a therapeutic strategy to target c-Myc. Cell 2011;146:904–917.
46. Filippakopoulos P, Qi J, Picaud S, et al. Selective inhibition of BET bromodomains. Nature 2010;468:1067–1073.
47. Kumar K, DeCant BT, Grippo PJ, et al. BET inhibitors block pancreatic stellate cell collagen I production and attenuate fibrosis in vivo. JCI Insight 2017;2:e88032.

Received December 22, 2023. Accepted August 5, 2024.

Correspondence
Address correspondence to: Mario A. Shields, PhD, Department of Pathology, Renaissance School of Medicine, Stony Brook University, 101 Nicolls Road, BST 9-150 Stony Brook, New York 11794. e-mail: mario.shields@stonybrook.edu; or Hidayatullah G. Munshi, MD, Department of Medicine, Northwestern University Feinberg School of Medicine, 303 East Superior Avenue, Lurie 3-117, Chicago, Illinois 60611. e-mail: h-munshi@northwestern.edu.

Acknowledgements
This work was supported by the Northwestern University Pathology Core Facility and the Northwestern University Center for Advanced Microscopy, both generously supported by NCI CCSG P30CA060553, awarded to the Robert H. Lurie Comprehensive Cancer Center. The authors thank Nida Mubin and Yaning Xi for their assistance with some of the experiments.

CRediT Authorship Contributions

Mario A. Shields, PhD (Conceptualization: Lead; Data curation: Lead; Formal analysis: Lead; Funding acquisition: Supporting; Investigation: Lead; Methodology: Lead; Project administration: Lead; Resources: Equal; Supervision: Equal; Validation: Lead; Visualization: Lead; Writing – original draft: Equal; Writing – review & editing: Equal)

Anastasia E. Metropulos, BSc (Data curation: Supporting; Investigation: Supporting; Methodology: Supporting; Writing – review & editing: Supporting)

Christina Spaulding (Data curation: Supporting; Investigation: Supporting; Writing – review & editing: Supporting)

Khulood A. Alzahrani (Data curation: Supporting)

Tomonori Hirose, MD, PhD (Resources: Supporting; Writing – review & editing: Supporting)

Shigeo Ohno, PhD (Resources: Supporting; Writing – review & editing: Supporting)

Thao N.D. Pham, PhD (Data curation: Supporting; Investigation: Supporting; Writing – review & editing: Supporting)

Hidayatullah G. Munshi, MD (Conceptualization: Lead; Data curation: Supporting; Formal analysis: Equal; Funding acquisition: Lead; Investigation: Equal; Methodology: Equal; Project administration: Lead; Resources: Lead; Supervision: Lead; Validation: Equal; Writing – original draft: Lead; Writing – review & editing: Lead)

Conflicts of interest

The authors disclose no conflicts.

Funding

This work was supported by grants R01CA217907 (to H.G.M.), R01CA283925 (to M.A.S.), a Merit award I01BX005595 (to H.G.M.) from the Department of Veterans Affairs, and APA/APA Foundation 2020 Young Investigator in Pancreatology Grant (to M.A.S.). The contents of this article are the responsibility of the authors and do not represent the views of the Department of Veterans Affairs or the United States Government.